

# IBM Research Report

## Effects of Under Bump Metallization and Nickel Alloying Element on the Undercooling Behavior of Sn-based, Pb-free Solders

Moon Gi Cho<sup>1</sup>, Sung K. Kang<sup>2</sup>, Sun-Kyoung Seo<sup>1</sup>,  
Da-Yuan Shih<sup>2</sup>, Hyuck Mo Lee<sup>1</sup>

<sup>1</sup>Department of Materials Science and Engineering  
KAIST  
335 Gwahangno, Yuseong-gu  
Deajon 305-701  
Republic of Korea

<sup>2</sup>IBM Research Division  
Thomas J. Watson Research Center  
P.O. Box 218  
Yorktown Heights, NY 10598



Research Division

Almaden - Austin - Beijing - Cambridge - Haifa - India - T. J. Watson - Tokyo - Zurich

Effects of Under Bump Metallization and Nickel Alloying Element on the Undercooling

Behavior of Sn-Based, Pb-free Solders

Moon Gi Cho, Sung K. Kang,\* Sun-Kyoung Seo, Da-Yuan Shih,\*

and Hyuck Mo Lee

Department of Materials Science and Engineering, KAIST

335 Gwahangno, Yuseong-gu,

Daejeon, Republic of Korea 305-701

\* IBM T.J. Watson Research Center

1101 Kitchawan Road, Route 134,

Yorktown Heights, NY 10598, USA

Corresponding Author: Prof. Hyuck Mo Lee

E-mail: hmlee@kaist.ac.kr

Tel: +82-42-869-3334

Fax: +82-42-869-3310

## Abstract

A significant reduction of the undercooling of Sn-based solder alloys was previously reported when they were reacted with various under bump metallurgies (UBMs). In the present study, new experiments have been designed and carried out to understand the undercooling behavior of various Cu- and Ni-doped solders on Ni UBM. Two competing mechanisms were further investigated that includes the formation of intermetallic compounds (IMCs) at solder/UBM interface and the change of solder composition due to the dissolution of Ni UBM into solder. Two types of IMCs, including both  $\text{Ni}_3\text{Sn}_4$  and  $\text{Cu}_6\text{Sn}_5$ , that were formed at the interface were correlated with the undercooling of Sn-0.2Cu and Sn-3.8Ag-0.2Cu solders. In addition, the compositional changes of various Sn-based solders after reactions with Ni UBM were analyzed. Based on the experimental results, it was found that the significant reduction in undercooling is primarily caused by dissolved Ni atoms from Ni UBM and the concurrent formation of  $\text{Ni}_3\text{Sn}_4$  IMC in the solder matrix. Finally, the beneficial effect of Ni dissolution is thermodynamic favorable as confirmed by the thermo-calculation and DSC measurements with various Ni-doped solder alloys.

**Key Words:** undercooling, Ni alloying element, Pb-free solder, under bump metallurgy,  
intermetallic compounds

## 1. Introduction

Near-eutectic binary or ternary Sn-based solder alloys are the promising Pb-free candidates to replace Pb-containing solders such as 37Pb-63Sn or 97Pb-3Sn in electronic packaging applications. The popularly used Sn-based solders include Sn-0.7Cu, Sn-3.5Ag and Sn-3.8Ag-0.7Cu (in weight percent unless specified otherwise). Since most Sn-based solders consist of more than 90 wt% Sn and a small amount of alloying additions such as Cu and Ag, the physical, chemical and mechanical properties are heavily affected by the unique body-centered tetragonal crystal structure of pure Sn.<sup>1</sup> The significant undercooling behavior of Sn-based solders clearly indicates one of such propensities that molten Sn solder is difficult to solidify. When Sn-based solders are solidified, the solidification does not occur readily even though the liquid phase passes its equilibrium phase transformation temperature. This phenomenon is called as “*undercooling*” and is attributed to the difficulty in nucleating a solid phase from a liquid phase.

In case of the pure Sn without any appreciable amount of doped impurities, the maximum undercooling observed was 107-120K.<sup>2,3</sup> The amount of undercooling in Sn-

based Pb-free solders was recently reported to be about 30°C, which is much larger than the undercooling of Pb-rich solders.<sup>4-6</sup> The large amount of the undercooling in Sn-based solders can influence their microstructures, such as Sn dendrite size, eutectic microstructure, formation of large primary phases such as Ag<sub>3</sub>Sn and Cu<sub>6</sub>Sn<sub>5</sub>,<sup>4,5</sup> and, thereby their mechanical properties.<sup>7,8</sup> In addition, a large amount of undercooling can have a serious bearing on the reliability of solder joints, such as in flip chip solder bumps, since random solidification in a full area array of many tiny solder bumps can cause an unfavorable situation in which some bumps already solidified while others not. This could lead to a higher stress concentration on the solidified bumps and cause early mechanical failures within solder joints.<sup>9</sup>

In order to reduce the undercooling of Sn-based solder alloys, it has been suggested to promote the nucleation of  $\beta$ -Sn phase by modifying solder composition and/or by adding impurity elements. It was reported that the undercooling was significantly reduced by adding minor alloying elements, such as Zn and Co.<sup>6,9</sup> When solder alloys are applied to a wettable surface such as under bump metallurgy (UBM) in electronic packaging, the amount of the undercooling of Sn-based solders was also reduced.<sup>8,9</sup> To understand why a wettable surface can reduce undercooling, a systematic

investigation has been conducted with various Pb-free solders (pure Sn, Sn-0.7Cu, Sn-3.5Ag and Sn-3.8Ag-0.7Cu) reflowed on UBMs such as Cu or Ni.<sup>8</sup> In the cases of pure Sn and Sn-3.5Ag solders, a very significant reduction in undercooling was obtained (about 20°C) by the reaction with Ni UBM, while about 10°C reduction with Cu UBM. In addition, in the Cu-containing solders (Sn-0.7Cu and Sn-3.8Ag-0.7Cu), the undercooling decreased by only about 10°C, independent of the UBMs (Cu vs. Ni). In our previous report, the different behavior of UBMs on the undercooling was explained in terms of IMCs ( $\text{Cu}_6\text{Sn}_5$  vs.  $\text{Ni}_3\text{Sn}_4$ ) formed at the interface, and suggested that the interfacial  $\text{Ni}_3\text{Sn}_4$  formed on Ni UBM would act as a favorable heterogeneous nucleation site. In another study, we have found an interesting result that a small addition of Ni into Sn-rich solders can also reduce the undercooling of Sn-2.0Ag, but not Sn-0.7Cu.<sup>10</sup>

In the present work, to explain the effects of UBMs and minor alloying elements on the undercooling behavior of Sn-based solders, several experiments were designed with Cu-containing solders reacted with Ni UBM and Ni-doped solders. The IMCs phases formed at the interface ( $\text{Ni}_3\text{Sn}_4$  vs.  $\text{Cu}_6\text{Sn}_5$ ) and the compositional changes in the solder matrix when reacted with Ni UBMs were investigated. In particular, to

clarify the relation between  $\text{Ni}_3\text{Sn}_4$  IMCs formed at the interface and the undercooling of Sn-based solders, Sn-0.2Cu and Sn-3.8Ag-0.2Cu solders were employed. It has been reported that, when the Cu content is more than 0.4 wt% in the solders,  $(\text{Cu,Ni})_6\text{Sn}_5$  forms on Ni-based UBMs, while,  $(\text{Ni,Cu})_3\text{Sn}_4$  forms when Cu is less than 0.4 wt%,<sup>11,12</sup>

In the present study, the 0.2 wt% Cu-containing solders are chosen to react with Ni UBM to form the  $\text{Ni}_3\text{Sn}_4$  type IMCs at the interface and to compare their undercooling with those on Cu UBM. In addition, the compositional changes of various Sn-based solders due to the dissolution of Ni UBMs during reflow are examined following the previous report that a Ni-doping can affect the undercooling.<sup>10</sup> Finally, to explain the beneficial effects of the Ni atoms dissolved from Ni UBMs on the undercooling of Sn-based solders, thermodynamic calculations and DSC measurement with various Ni-doped solders are conducted.

## **2. Experimental Procedures**

The solder compositions used in this experiment are Sn-0.2Cu and Sn-3.8Ag-0.2Cu, which were produced in our laboratory. Each solder composition was prepared from high purity (>99.99%) Sn, Ag, Cu elemental mixtures encapsulated under



vacuum in a quartz tube, and then melted at about 1000°C or higher. Electroplated Cu and Ni UBMs were employed. The thicknesses of electroplated Cu and Ni were 20 μm and 10 μm, respectively. Approximately, the same substrate size (1 mm x 1 mm) of different UBMs and solder weight (4.8 mg, d=1050 μm) were used to eliminate any effects due to the variations in solder volume and substrate area. Interfacial reaction experiments were conducted by reflowing the same amount of a solder on a substrate on a hotplate at 260°C for 10 sec with a rosin-activated (RA) flux. Subsequently, differential scanning calorimetry (DSC) experiment was performed in a Diamond DSC calorimeter (Perkin-Elmer, Inc., USA), which was heated and cooled at a rate of 6°C/min under a nitrogen atmosphere with the substrate plus solder.

To examine the effects of the Ni atoms on the undercooling of Sn-based solders, various high purity Ni-doped solder alloys, such as Sn-0.2Ni, Sn-3.5Ag-0.1Ni, Sn-3.5Ag-0.15Ni, Sn-0.7Cu-0.2Ni and Sn-0.7Cu-0.4Ni, were produced in our laboratory. The doping level of the Ni alloying element was determined by the thermodynamic calculations. The detailed calculations are described in a next section. DSC measurements with the Ni-doped solder alloys were conducted in the same way.

After DSC experiments, the microstructures of the reflowed solders and the interface with a substrate were examined by cross-sectioning, polishing, optical microscopy (OM) and scanning electron microscopy (SEM). The back-scattered electron mode of SEM was used to observe the IMCs. Energy-dispersive X-ray spectroscopy (EDS) and X-ray diffractometry (XRD) using Cu  $K\alpha_1$  were used to identify IMC phases. Electron probe micro-analyzer (EPMA) was used to analyze the compositional changes in the solders after the interfacial reactions with UBMs.

### **3. Results and Discussion**

#### ***IMCs formation and DSC Results of 0.2 wt% Cu-containing Solders***

Figure 1 shows the SEM images of the interface between two solders and two UBMs (Ni vs. Cu). IMCs formed at the interface were analyzed by EDS to obtain their chemical compositions. The scallop-like  $\text{Cu}_6\text{Sn}_5$  IMC was commonly observed at the interface between all solders and Cu UBM, and  $\text{Cu}_3\text{Sn}$  was occasionally found. Meanwhile, IMCs formed on Ni UBMs were much thinner than  $\text{Cu}_6\text{Sn}_5$ , which were identified as the ternary Sn-Cu-Ni compounds of Sn (58-59 at%), Cu (5-6 at%) and Ni (36-37 at%) by EDS. The ternary IMC is believed to be  $(\text{Ni,Cu})_3\text{Sn}_4$  with Cu substitution calculated by their atomic ratios. This is consistent with the previous observations when Pb-free solders containing less than 0.4 wt% Cu reacted with Ni

UBM during reflow.<sup>11,12</sup> Therefore, it is expected that the undercooling of two 0.2 wt% Cu-containing solders with Ni UBM would be significantly reduced (down to less than 10°C), according to our previous suggestion that the interfacial Ni<sub>3</sub>Sn<sub>4</sub> formed on Ni UBM would act as a favorite heterogeneous nucleation site of  $\beta$ -Sn phases.<sup>8</sup>

Figure 2 depicts a typical DSC thermal profile recorded during heating and cooling of a Sn-based solder. Peak and onset temperatures in heating and cooling curves were measured from Fig. 2. In this study, the amount of undercooling was defined by the difference of two onset temperatures in heating and cooling curves, because they describe better the physical process occurring during melting and solidification.

Table 1 summarizes the DSC results obtained from two solder alloys with or without UBMs. For each solder, the onset and peak temperatures of the thermal profile were recorded with two different UBMs. The amount of undercooling estimated by the difference of onset temperatures was listed for each case. For the bulk solders without UBMs, the undercooling was 35.1°C for Sn-0.2Cu and 32°C for Sn-3.8Ag-0.2Cu. When both solders were reacted with Cu or Ni UBMs, the amount of undercooling in Sn-0.2Cu was reduced to 19.3°C on Cu UBM, and 15.3°C on Ni UBM, respectively. In

case of Sn-3.8Ag-0.2Cu, it was also decreased to 14.3°C with Cu and 15.8°C with Ni UBM. The beneficial effect of Cu or Ni UBMs in reducing the undercooling of Sn-based solders is consistent with our previous work.<sup>8</sup> However, there was no big difference in the amount of the undercooling reduced between Cu and Ni UBM.

Table 2 summarizes the amount of undercooling and IMC phases formed at the interface observed in the previous and present works. In our previous study, a large decrease of undercooling in pure Sn and Sn-3.5Ag with Ni UBMs was observed, and it was suggested that Ni-Sn type IMCs formed at the interface was more effective than Cu-Sn type IMCs in reducing the amount of undercooling by acting as a favorite heterogeneous nucleation site.<sup>8</sup> However, in the present study, the undercooling of the Cu-containing solders (Sn-0.2Cu and Sn-3.8Ag-0.2Cu) with Ni UBM was not much different from that of Cu UBM even though Ni-Sn type IMCs formed at the interface with Ni UBM. It implies that the type of IMC phase formed at the interface between a solder and UBM is not the major factor to reduce the undercooling of Sn-rich solders.

### ***Compositional Changes in Sn-based Solders during Reflow***

In general, the solder composition is changed by the dissolution of UBMs into

the solder during reflow. In the case of pure Sn, the changes in the microstructures are observed depending on the Cu vs. Ni UBM, as shown in Fig. 3. When the compositional analysis was performed in an area of 50  $\mu\text{m}$  x 50  $\mu\text{m}$  by EPMA, the composition of the pure Sn changed to the near-eutectic binary Sn-Cu composition after reaction with Cu UBM, which consists of 99.1-99.2 wt% Sn and 0.8-0.9 wt% Cu. In the case of Ni UBM, the pure Sn changed to a near-eutectic composition of 99.91-99.9 wt% Sn and 0.09-0.1 wt% Ni.

The dissolution of UBMs during reflow is also common in other Sn-based solders, such as Sn-0.2Cu, Sn-0.7Cu, Sn-3.5Ag and Sn-3.5Ag-0.7Cu. Figure 4 is the representative OM images of Sn-3.5Ag, Sn-0.7Cu, and Sn-0.2Cu reacted with Ni UBM. Note that  $\text{Ni}_3\text{Sn}_4$  was formed at the interface of the Sn-3.5Ag and Ni UBM during reflow,  $(\text{Cu,Ni})_6\text{Sn}_5$  in Sn-0.7Cu, and  $(\text{Ni,Sn})_3\text{Sn}_4$  in Sn-0.2Cu. The microstructure of Sn-3.5Ag reacted with Ni UBM consists of  $\beta$ -Sn dendrites (light contrast) and the eutectic microstructure (dark contrast, a mixture of fine intermetallic particles in the Sn matrix). For Sn-0.7Cu and Sn-0.2Cu reacted with Ni UBM, the  $\beta$ -Sn dendrites and the eutectic microstructure were also observed inside the solder far from the interface. However, a few needle-like IMCs were found in the Sn-3.5Ag reacted with Ni UBM, but not in the Sn-0.7Cu and Sn-0.2Cu. The needle-like IMCs were too thin to be

identified quantitatively by EDS, but qualitatively confirmed to be the Ni-Sn binary IMCs.

EPMA mapping of the microstructure of Sn-3.5Ag with Sn-0.2Cu solders are shown in Figure 5 after reaction with Ni UBM, in areas far from the interface. Consistent with the previous analysis by EDS, the needle-like IMC in the Sn-3.5Ag was verified as a Ni-Sn binary IMC. In general, there are three equilibrium IMC phases existing, such as  $\text{Ni}_3\text{Sn}_4$ ,  $\text{Ni}_3\text{Sn}_2$  and  $\text{Ni}_3\text{Sn}$ , in the Ni-Sn binary phase diagram.<sup>13</sup> The  $\text{Ni}_3\text{Sn}_4$  is the most common phase in a reaction between Sn-rich solders and Ni UBM.<sup>8,14,15</sup> Therefore, the needle-like Ni-Sn IMCs appear to be  $\text{Ni}_3\text{Sn}_4$  IMCs. For the Sn-0.2Cu, the distribution of Ni atoms was much different from that of the Sn-3.5Ag, as shown in Fig. 5. Ni atoms were largely observed in the interdendritic area (of the eutectic microstructure), matching the distribution of Cu atoms. The Cu atoms react with Sn atoms to form fine  $\text{Cu}_6\text{Sn}_5$  IMC particles in the interdendritic area. Hence, it seems that the dissolved Ni atoms in the Sn-0.2Cu solder do not form the binary Ni-Sn IMCs, but the ternary phase of  $(\text{Cu},\text{Ni})_6\text{Sn}_5$  with the substitution of some Ni for Cu. In addition, when a compositional analysis was performed in an area of  $50\ \mu\text{m} \times 50\ \mu\text{m}$  by EPMA, 0.1-0.15 wt% Ni was detected inside the Sn-3.5Ag solder with Ni UBM, while

a much lower Ni content (0.01-0.03 wt%) was detected in the solder matrix of the Sn-0.2Cu and Sn-0.7Cu reacted with Ni UBM.

On the basis of this compositional analysis, the significant reduction of undercooling observed in pure Sn and Sn-3.5Ag with Ni UBM would be related to the Ni atoms dissolved from Ni UBM during reflow. In other words, when the dissolved Ni atoms react with Sn atoms to form  $\text{Ni}_3\text{Sn}_4$  inside the solders during solidification, the undercooling would be significantly reduced. On the other hand, in the Sn-0.7Cu and Sn-3.8Ag-0.7Cu with Ni UBMs, the amount of the dissolved Ni atoms during reflow is much lower than in pure Sn and Sn-3.5Ag. Moreover, the dissolved Ni atoms do not form  $\text{Ni}_3\text{Sn}_4$ , but  $(\text{Cu,Ni})_6\text{Sn}_5$  IMCs during solidification. Accordingly, the effect of the dissolved Ni atoms on the undercooling would be eliminated in the Cu-containing solders (Sn-0.7Cu or Sn-3.8Ag-0.7Cu) due to the formation of  $(\text{Cu,Ni})_6\text{Sn}_5$ .

### ***Thermodynamic Calculations of the Ni Solubility in Sn-based Solders***

Thermodynamic calculations were performed to quantitatively estimate the amount of the Ni atoms dissolved from Ni UBMs during reflow. Figure 6(a) is the equilibrium phase diagram of a Sn-Ni binary system and Fig. 6(b) is a pseudo-binary

phase diagram of Sn-3.5Ag vs. Ni, which is the vertical section of the Sn-Ag-Ni ternary phase diagram calculated along a constant ratio of Sn/Ag (96.5:3.5 in wt%). The solubility limit of Ni in the pure Sn and Sn-3.5Ag solders is 0.198 wt% and 0.101 wt% at 250°C, respectively. In other words, 0.198 wt% and 0.101 wt% Ni can be dissolved into pure Sn and Sn-3.5Ag, respectively, during the interfacial reaction with Ni UBM at 250°C. In addition, it is confirmed that most of the dissolved Ni atoms precipitate out as the primary Ni<sub>3</sub>Sn<sub>4</sub> IMC inside the solders during solidification, as shown in Figs 6(a) and 6(b).

In case of the Sn-0.7Cu, the similar thermodynamic calculation can be applied to estimate the amount of the dissolved Ni and a primary phase during solidification. However, there is no reliable data available for the equilibrium phase diagram of the Sn-Cu-Ni ternary system. Especially, it is still in dispute whether a Sn-Cu-Ni ternary IMC exists in a Sn-rich side or not. Thus, instead of the equilibrium phase diagram, the solubility limit of Ni in Sn-0.7Cu was approximated using the experimental isothermal section of the Sn-Cu-Ni ternary system at 240°C.<sup>11,16-21</sup> As shown in Fig. 7, the amount of the dissolved Ni in Sn-0.7Cu is estimated to be about 0.04 wt%, which is much lower than in pure Sn and Sn-3.5Ag. In addition, when the 0.04 wt% Ni is dissolved into the



Sn-0.7Cu solder, the primary phase is a  $\text{Cu}_6\text{Sn}_5$  type IMC. These calculations are in agreement with our previous experimental observations. However, it is noted that if the amount of Ni content in Sn-0.7Cu exceeds about 0.3 wt% (as shown in Fig. 7),  $\text{Ni}_3\text{Sn}_4$  IMCs can form as a primary phase during solidification.

### ***Ni Alloying Effect on Reducing the Undercooling of Solders***

Based on the previous thermodynamic calculations, further investigation has been conducted to find the Ni alloying effect on the undercooling of Sn-rich solders. Various Ni-doped solder alloys, such as Sn-0.2Ni, Sn-3.5Ag-0.1Ni, Sn-3.5Ag-0.15Ni, Sn-0.7Cu-0.2Ni and Sn-0.7Cu-0.4Ni were prepared similarly described in the experimental procedure. In Sn-0.2Ni and Sn-3.5Ag-0.1Ni, the amount of the Ni content matches to the solubility limit in each solder at 250°C. In case of the Sn-0.7Cu solders, the Ni content was over the solubility limit, especially up to 0.4 wt%, to form  $\text{Ni}_3\text{Sn}_4$  IMCs inside the solders during solidification, which would result in the reduction of the undercooling.

Table 3 summarizes the DSC results obtained from the five Ni-doped solder alloys, comparing with our previous results. The undercooling of pure Sn (31.2°C) was

significantly reduced to 9.1°C by the reaction with Ni UBM. In addition, an equivalent amount of the decrease in the undercooling was also obtained by adding 0.2 wt% Ni to pure Sn. For the Sn-3.5Ag solders, a similar trend was also noted, but a significant reduction at the Ni doping level of 0.15 wt%, not 0.1 wt%. In addition, the microstructures of two solders (Sn-0.2Ni and Sn-3.5Ag-0.15Ni) exhibit a few needle-like  $\text{Ni}_3\text{Sn}_4$  IMCs, as shown in Fig. 8. This microstructure is consistent with those observed in the pure Sn and Sn-3.5Ag reacted with Ni UBM (Fig. 4). Furthermore, the experimental results of both the undercooling and the microstructures of the Ni-doped solders (Sn-0.2Ni and Sn-3.5Ag-0.15Ni) support our hypothesis: the significant reduction of the undercooling in pure Sn and Sn-3.5Ag reacted on Ni UBM would be related to the dissolved Ni atoms from Ni UBM and thereby owing to the formation of  $\text{Ni}_3\text{Sn}_4$  IMCs in the solder matrix (not at the interface) during their solidification.

For Sn-0.7Cu, when 0.2 wt% Ni was added, the undercooling was reduced to 14.5°C, which is still larger than the undercooling of Sn-0.2Ni and Sn-3.5Ag-0.15Ni. However, when the Ni content increased to 0.4 wt%, the undercooling of the Sn-0.7Cu significantly decreased to 9.6°C, and the amount of the reduction was as much as those observed in Sn-0.2Ni and Sn-3.5Ag-0.15Ni. Figure 8 shows the microstructures of two

Ni-doped Sn-Cu solders after DSC experiments. The microstructure of the Sn-0.7Cu-0.2Ni consists of the  $\beta$ -Sn dendrites and the eutectic microstructure. However, in the Sn-0.7Cu-0.4Ni,  $\beta$ -Sn dendrites were not observed, but only the needle-like IMCs dispersed in the matrix. It is interesting that the microstructure of Sn-0.7Cu-0.2Ni is similar to the Sn-Cu solders (Sn-0.2Cu and Sn-0.7Cu) reacted with Ni UBM, while the microstructure of Sn-0.7Cu-0.4Ni is similar to the pure Sn reacted with Ni UBM. Moreover, the needle-like IMCs observed in Sn-0.7Cu-0.4Ni are very similar to the  $\text{Ni}_3\text{Sn}_4$  IMCs observed inside the Sn-0.2Ni and pure Sn reacted with Ni UBM. In order to identify the IMC phases formed in Sn-0.7Cu-0.2Ni vs. Sn-0.7Cu-0.4Ni, an XRD analysis was conducted. As shown in Fig. 9, several peaks with a high intensity and a few small peaks were detected commonly in both solders. The peaks with the high intensity in both solders were identified as Sn. The small peaks of the Sn-0.7Cu-0.2Ni matched with  $\text{Cu}_6\text{Sn}_5$  IMCs, while, in case of Sn-0.7Cu-0.4Ni, identified as  $\text{Ni}_3\text{Sn}_4$ . Therefore, the formation of  $\text{Ni}_3\text{Sn}_4$  was verified in Sn-0.7Cu-0.4Ni with a small amount of undercooling ( $9.6^\circ\text{C}$ ), while the formation of  $\text{Cu}_6\text{Sn}_5$  (not  $\text{Ni}_3\text{Sn}_4$ ) in Sn-0.7Cu-0.2Ni with a large amount of undercooling ( $14.5^\circ\text{C}$ ) was confirmed. These experimental results of the Ni-doped Sn-Cu solders clearly support the above-mentioned hypothesis. Moreover, it is also demonstrated that if the amount of the Ni content in the Sn-Cu

solder is not enough to form  $\text{Ni}_3\text{Sn}_4$  IMCs inside the solder, the beneficial effect of Ni addition on the undercooling can be eliminated owing to the formation of  $(\text{Cu},\text{Ni})_6\text{Sn}_5$  IMCs.

The large reduction of the undercooling observed in pure Sn and Sn-3.5Ag solders reacted with Ni UBM is now attributed to the metallurgical effect of Ni atoms dissolved from Ni UBM, which is often displayed by the accompanying formation of  $\text{Ni}_3\text{Sn}_4$  IMCs in the solder matrix during solidification. In addition, the undercooling of Sn-based solders can be reduced by the reaction with UBMs, but a careful compositional adjustment is needed to properly achieve the beneficial effect.

#### **4. Summary**

In the present work, in order to explain the large reduction of the undercooling (down to less than  $10^\circ\text{C}$ ) observed in pure Sn and Sn-3.5Ag when reacted with Ni UBM, new experiments and thermodynamic calculations were performed with both 0.2Cu-containing and Ni-doped Sn-based solders. The corresponding IMCs phases ( $\text{Ni}_3\text{Sn}_4$  vs.  $\text{Cu}_6\text{Sn}_5$ ) formed at the interface and the composition changes in the solder matrix due to the reaction with UBMs were characterized.

Firstly, the relation between the formation of  $\text{Ni}_3\text{Sn}_4$  at the interface and undercooling of Sn-based solders was systematically investigated with the Cu-containing solders (Sn-0.2Cu and Sn-3.8Ag-0.2Cu). When the solders reacted with Ni UBM, the  $(\text{Ni,Cu})_3\text{Sn}_4$  phase was formed at the interface during reflow. However, the undercooling of Sn-0.2Cu or Sn-3.8Ag-0.2Cu reacted on Ni UBM was not much different with Cu UBM. Therefore, it was found that the type of IMC phase formed at the interface is not a primary contributing factor to yield a significant reduction of the undercooling in the presence of different UBMs.

By observing the microstructures of the pure Sn, Sn-3.5Ag, Sn-0.7Cu and Sn-0.2Cu reacted with Ni UBMs, it was found that the significant reduction of the undercooling (down to less than  $10^\circ\text{C}$ ) was related to the Ni atoms dissolved from Ni UBM and the concurrent formation of  $\text{Ni}_3\text{Sn}_4$  IMCs in the solder matrix, not at the interface.

The metallurgical effect of the dissolved Ni on the undercooling was further proven by the thermodynamic calculations and DSC measurements with various Ni-

doped solder alloys (Sn-0.2Ni, Sn-3.5Ag-0.15Ni, Sn-0.7Cu-0.2Ni and Sn-0.7Cu-0.4Ni). The large reduction of the undercooling when reacted with Ni UBM is attributed to the metallurgical effect of Ni atoms dissolved from Ni UBM, which is displayed by accompanying the formation of  $\text{Ni}_3\text{Sn}_4$  inside the solder during solidification. Moreover, in case of the Sn-Cu solders reacted with Ni UBM, the beneficial effect of the dissolved Ni is largely eliminated when most Ni atoms are used to form  $(\text{Cu},\text{Ni})_6\text{Sn}_5$ . For example, in case of Sn-0.7Cu, the addition of 0.2 wt% Ni is not enough to obtain a significant reduction in the undercooling, while 0.4 wt% Ni is good enough to achieve this purpose by forming  $\text{Ni}_3\text{Sn}_4$  IMCs in the solder matrix.

In conclusion, it is found that the undercooling of Sn-based Pb-free solders can be reduced by the presence of wettable UBMs. Depending on the solder composition, a carefully controlled composition is required to achieve this purpose.,.

### **Acknowledgements**

We appreciate very much Drs. Hae Jin Kim and Jin Bae Lee at the Korea Basic Science Institute (KBSI) for their work on DSC measurements as well as Han-Na Park in KBSI for the SEM observation and EDS analysis.

## References

1. S.K. Kang, P. Lauro, D.Y. Shih, D.W. Henderson and K.J. Puttlitz: The microstructure,

solidification, mechanical properties, and thermal fatigue behavior of lead (Pb)-free solders and solder joints used in microelectronic applications. *IBM J. Res. Dev.* 49(4/5), 607 (2005).

2. B. Vonnegut: Variation with temperature of the nucleation rate of supercooled liquid tin and water drops. *J. Colloid. Sci.* 3, 563 (1948).

3. G.M. Pound and V.K. LA Mer: Kinetics of crystalline nucleus formation in supercooled liquid tin. *J. Amer. Chem. Soc.* 74, 2323 (1952).

4. S.K. Kang, W.K. Choi, D.-Y. Shih, D.W. Henderson, T. Gosselin, A. Sarkhel, C. Goldsmith and K.J. Puttlitz: Formation of  $\text{Ag}_3\text{Sn}$  plates in Sn-Ag-Cu alloys and optimization of their alloy composition, in *Proc. 53rd Electronic Components and Technology Conference* (Piscataway, NJ: IEEE, 2003), pp. 64-70.

5. L.P. Lehman, R.K. Kinyanjui, L. Zavalij, A. Zribi and E.J. Cotts: Growth and selection of intermetallic species in Sn-Ag-Cu no-Pb solder systems based on pad metallurgies and thermal histories, in *Proc. 53rd Electronic Components and Technology Conference* (Piscataway, NJ: IEEE, 2003), pp. 1215-1221.

6. S.K. Kang, D.-Y. Shih, D. Leonard, D.W. Henderson, T. Gosselin, S.-I. Cho, J. Yu and W.K. Choi: Controlling  $\text{Ag}_3\text{Sn}$  plate formation in near-ternary-eutectic Sn-Ag-Cu solder by minor Zn alloying. *JOM* 56(6), 34 (2004).



7. Q. Xiao, L. Nguyen and W.D. Armstrong: The anomalous microstructural, tensile, and aging response of thin-cast Sn<sub>3.9</sub>Ag<sub>0.6</sub>Cu lead-free solder. *J. Electron. Mater.* 34(5), 617 (2005).
8. M.G. Cho, S.K. Kang and H.M. Lee: Undercooling and microhardness of Pb-free solders on various under bump metallurgies. *J. Mater. Res.* 23(4), 1147 (2008).
9. S.K. Kang, M.G. Cho, P. Lauro and D.-Y. Shih: Critical factors affecting the undercooling of Pb-free, flip-chip solder solder bumps and in-situ observation of solidification process, in *Proc. 57th Electronic Components and Technology Conference* (Piscataway, NJ: IEEE, 2007), pp. 1597-1603.
10. S.K. Kang, M.G. Cho, D.-Y. Shih, S.-K. Seo and H.M. Lee: Controlling the Interfacial Reactions in Pb-free Interconnections by Adding Minor Alloying Elements to Sn-rich Solders, in *Proc. 58th Electronic Components and Technology Conference* (Piscataway, NJ: IEEE, 2008), pp. 478-484.
11. C.E. Ho, S.C. Yang and C.R. Kao: Interfacial reaction issues for lead-free electronic solders. *J. Mater. Sci.: Mater. Electron.* 18, 155 (2007).
12. S.-W. Chen and C.-H. Wang: Interfacial reactions of Sn-Cu/Ni couples at 250°C. *J. Mater. Res.* 21(9), 2270 (2006).
13. G. Ghosh: Thermodynamic modeling of the nickel-lead-tin system. *Metall. Mater.*

*Trans. A* 30A, 1481 (1999).

14. J.H. Kim, S.W. Jeong, H.D. Kim and H.M. Lee: Morphological transition of interfacial  $\text{Ni}_3\text{Sn}_4$  grains at Sn-3.5Ag/Ni joint. *J. Electron. Mater.* 32(11), 1228 (2003).

15. W.K. Choi and H.M. Lee: Prediction of primary intermetallic compound formation during interfacial reaction between Sn-based solder and Ni substrate. *Scripta Mater.* 46(11), 777 (2002).

16. K. Zeng, V. Vuorinen and J.K. Kivilahti: Interfacial reactions between lead-free SnAgCu solder and Ni(P) surface finish on printed circuit boards. *IEEE Trans. Electron. Packag. Manufact.* 25, 162 (2002).

17. T. Laurila, V. Vuorinen and J.K. Kivilahti: Interfacial reactions between lead-free solders and common base materials. *Mater. Sci. Eng.* R49, 1 (2005).

18. K. Zeng and K.N. Tu: Six cases of reliability study of Pb-free solder joints in electronic packaging technology. *Mater. Sci. Eng.* R38, 55 (2002).

19. T.B. Massalski (ed.): Binary Alloy Phase Diagrams. (ASM International, Metal Park, OH, 1990), pp. 1481.

20. K.-W. Moon, W.J. Boettinger, U.R. Kattner, F.S. Biancaniello and C.A. Handwerker: Experimental and thermodynamic assessment of Sn-Ag-Cu solder alloys. *J. Electron. Mater.* 29, 1122 (2000).

21. P. Nash and A. Nash: The Ni-Sn system. *Bull. Alloy Phase Diag.* 6, 350 (1985).

Table 1. DSC results for undercooling of Sn-0.2Cu and Sn-3.8Ag-0.2Cu with or without UBMs.

composition (wt %)	onset temp (heating) ( $T_1$ )	onset temp. (cooling) ( $T_2$ )	$\Delta T$ ( $T_1-T_2$ )	peak temperature*	
Sn-0.2Cu	only bulk	227.8°C	192.7°C	35.1	231.7 (H), 192.8 (C)
	on Cu	227.8°C	208.5°C	19.3	229.9 (H), 208.4 (C)
	on Ni	228.0°C	212.7°C	15.3	233.5 (H), 212.6 (C)
Sn-3.8Ag- 0.2Cu	only bulk	217.8°C	185.8°C	32	221.9 (H), 185.8 (C)
	on Cu	218.0°C	203.7°C	14.3	219.9 (H), 203.6 (C)
	on Ni	218.5°C	202.7°C	15.8	222.6 (H), 202.6 (C)

\*H stands for heating and C for cooling.

Table 2. The comparison of the amount of undercooling vs. IMCs formed at the interface phases obtained in our previous [Ref. 8] and present works.

composition (wt %)		Cu UBM	Ni UBM	comment
Pure Sn (31.2°C)	IMC*	$\text{Cu}_6\text{Sn}_5$	$\text{Ni}_3\text{Sn}_4$	ref. 8
	$\Delta T^{**}$	17.1°C	9.1°C	
Sn-0.2Cu (35.1°C)	IMC*	$\text{Cu}_6\text{Sn}_5$	$(\text{Ni,Cu})_3\text{Sn}_4$	-
	$\Delta T^{**}$	19.3°C	15.3°C	
Sn-0.7Cu (28.8°C)	IMC*	$\text{Cu}_6\text{Sn}_5$	$(\text{Cu,Ni})_6\text{Sn}_5$	ref. 8
	$\Delta T^{**}$	21.2°C	18.7°C	
Sn-3.5Ag (29.6°C)	IMC*	$\text{Cu}_6\text{Sn}_5$	$\text{Ni}_3\text{Sn}_4$	ref. 8
	$\Delta T^{**}$	16.1°C	10.9°C	
Sn-3.8Ag-0.2Cu (32°C)	IMC*	$\text{Cu}_6\text{Sn}_5$	$(\text{Cu,Ni})_6\text{Sn}_5$	-
	$\Delta T^{**}$	14.3°C	15.8°C	
Sn-3.8Ag-0.7Cu (24.6°C)	IMC*	$\text{Cu}_6\text{Sn}_5$	$(\text{Cu,Ni})_6\text{Sn}_5$	ref. 8
	$\Delta T^{**}$	20.7°C	17.4°C	

\*IMC phase formed at the interface between solders and UBMs.  
\*\*The amount of the undercooling reduced by the interfacial reaction with each UBM.

Table 3. DSC results for undercooling of the five Ni-doped solder alloys (Sn-0.2Ni, Sn-3.5Ag-0.1Ni, Sn-3.5Ag-0.15Ni, Sn-0.7Cu-0.2Ni and Sn-0.7Cu-0.4Ni), comparing with the previous results [Ref. 8].

composition (wt %)		onset temp. (heating) (T <sub>1</sub> )	onset temp. (cooling) (T <sub>2</sub> )	$\Delta T$ (T <sub>1</sub> -T <sub>2</sub> )	peak temperature*	comment
Pure Sn	only bulk	232.3°C	201.1°C	31.2	234 (H), 201.2 (C)	ref. 8
	on Ni	232.1°C	223.0°C	9.1	234.9 (H), 222.8 (C)	
Sn-0.2Ni		231.2°C	220.5°C	10.7	232.8 (H), 220.4 (C)	-
Sn-3.5Ag	only bulk	222.1°C	192.5°C	29.6	223.7 (H), 192.5 (C)	ref. 8
	on Ni	221.5°C	210.6°C	10.9	224.7 (H), 210.2 (C)	
Sn-3.5Ag-0.1Ni		221.2°C	203.9°C	17.3	222.4 (H), 203.9 (C)	-
Sn-3.5Ag-0.15Ni		220.9°C	213.5°C	7.4	222.3 (H), 213.2 (C)	-
Sn-0.7Cu	only bulk	229.6°C	200.3°C	28.8	230.3 (H), 202.3 (C)	ref. 8
	on Ni	227.5°C	208.8°C	18.7	230.6 (H), 208.7 (C)	
Sn-0.7Cu-0.2Ni		228.8°C	214.3°C	14.5	230.9 (H), 214.3 (C)	-
Sn-0.7Cu-0.4Ni		231.2°C	221.6°C	9.6	232.5 (H), 221.5 (C)	-

\*H stands for heating and C for cooling.

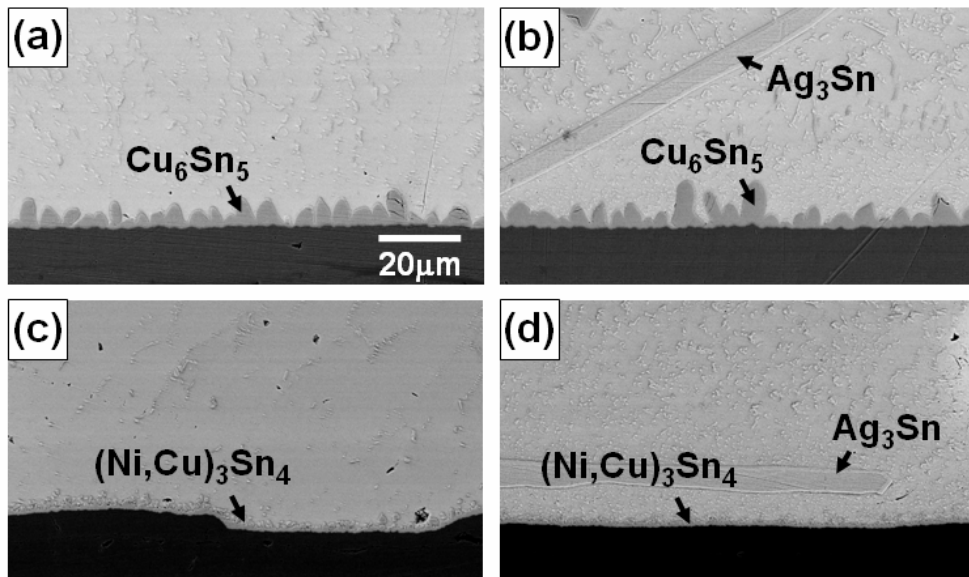


Figure 1. SEM images of the interface area between (a) Sn-0.2Cu solder and Cu UBM, (b) Sn-3.8Ag-0.2Cu solder and Cu UBM, (c) Sn-0.2Cu solder and Ni UBM, and (d) Sn-3.8Ag-0.2Cu solder and Ni UBM after reflow.

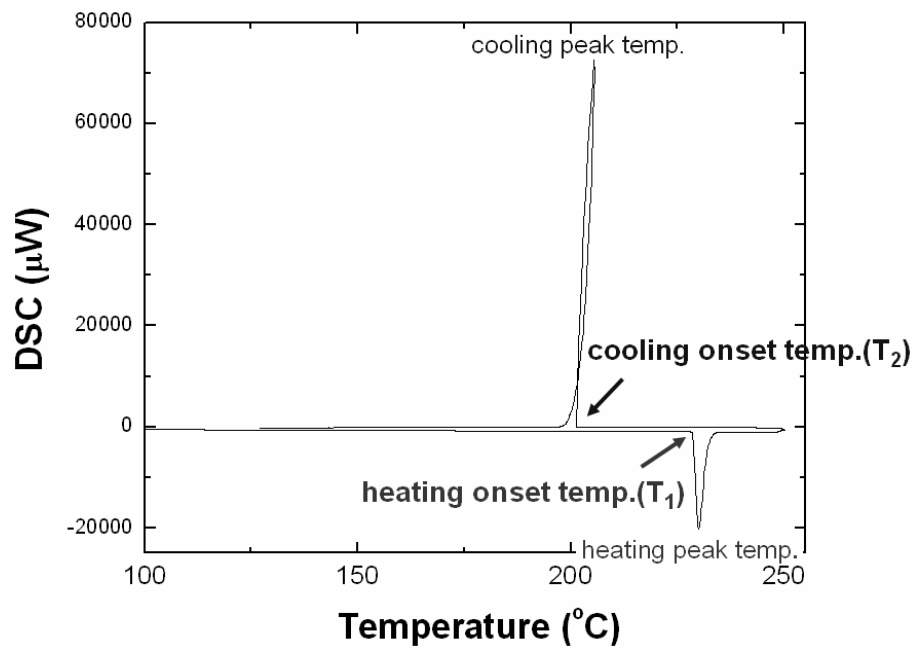


Figure 2. A typical DSC thermal profile recorded during heating and cooling of a Sn-based solder.



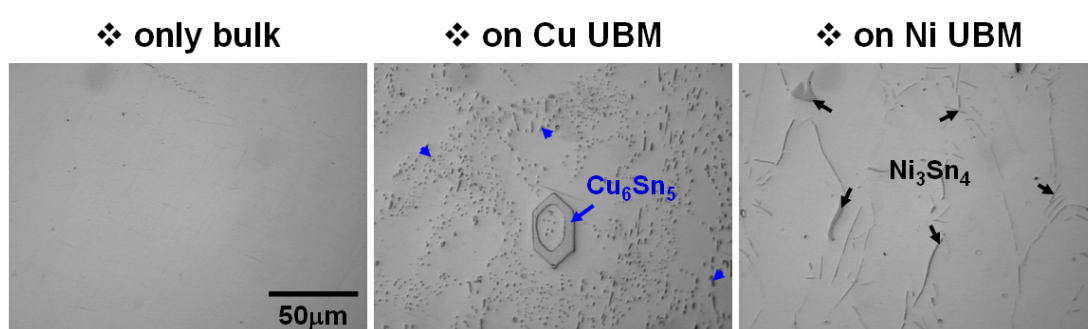


Figure 3. OM images inside the pure Sn with or without UBMs solidified at a cooling rate of 6°C/min during DSC.

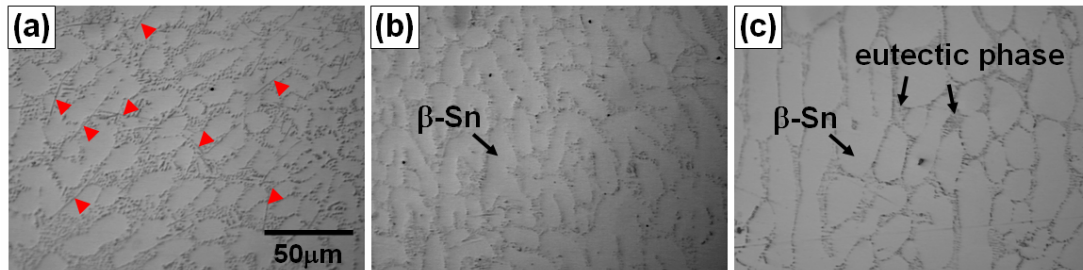


Figure 4. OM images inside (a) Sn-3.5Ag solder with Ni UBM, (b) Sn-0.7Cu solder with Ni UBM, and (c) Sn-0.2Cu solder with Ni UBM solidified at a cooling rate of 6°C/min during DSC.

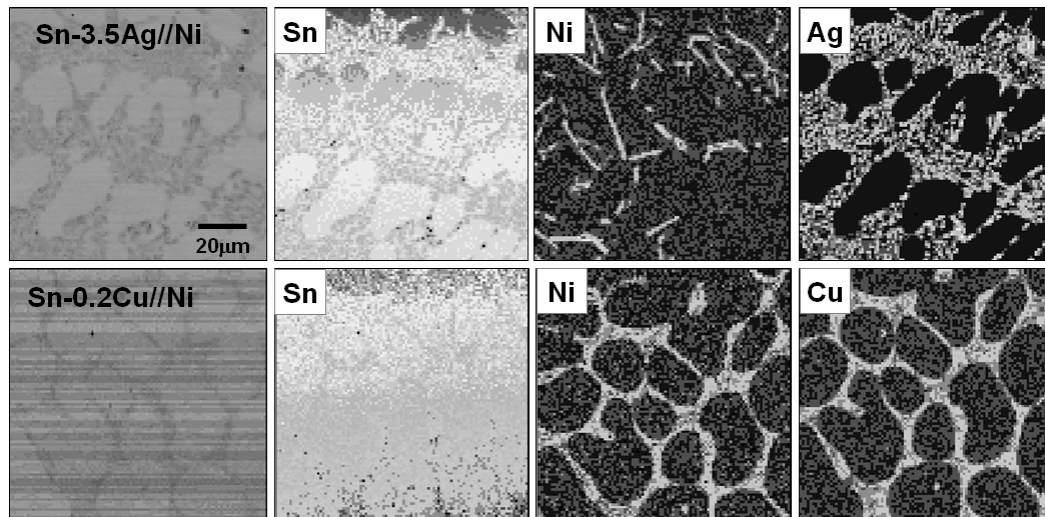


Figure 5. EPMA mapping images of the Sn-3.5Ag and Sn-0.2Cu solder inside reacted with Ni UBM.

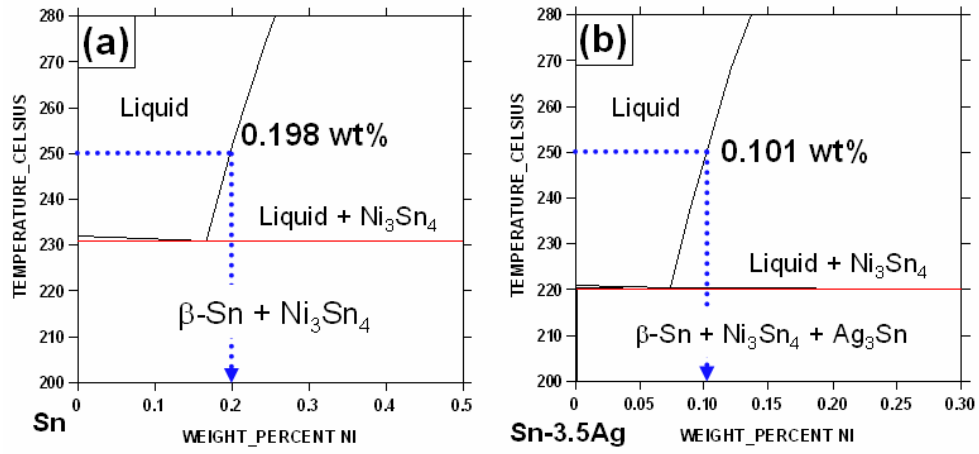


Figure 6. (a) The equilibrium phase diagram of a Sn-Ni binary system and (b) The vertical section of the Sn-Ag-Ni ternary phase diagram calculated along a constant 96.5:3.5 ratio of Sn/Ag (in wt%).

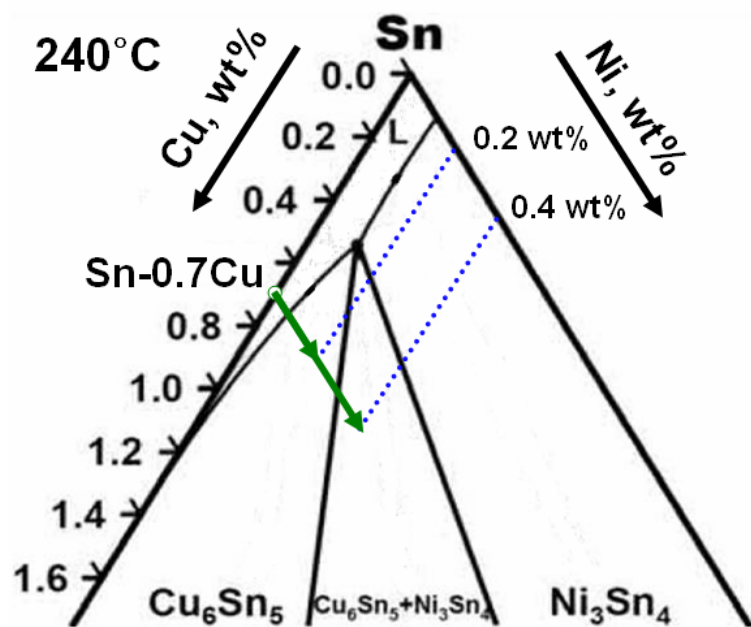


Figure 7. The experimental isothermal section of the Sn-rich region in the Sn-Cu-Ni ternary system at 240°C. This isothermal section is drawn based on the previously published works [Ref. 15-17] and the solubility data from the Cu-Sn [Ref. 18-19] and Ni-Sn [Ref. 20] binary systems.

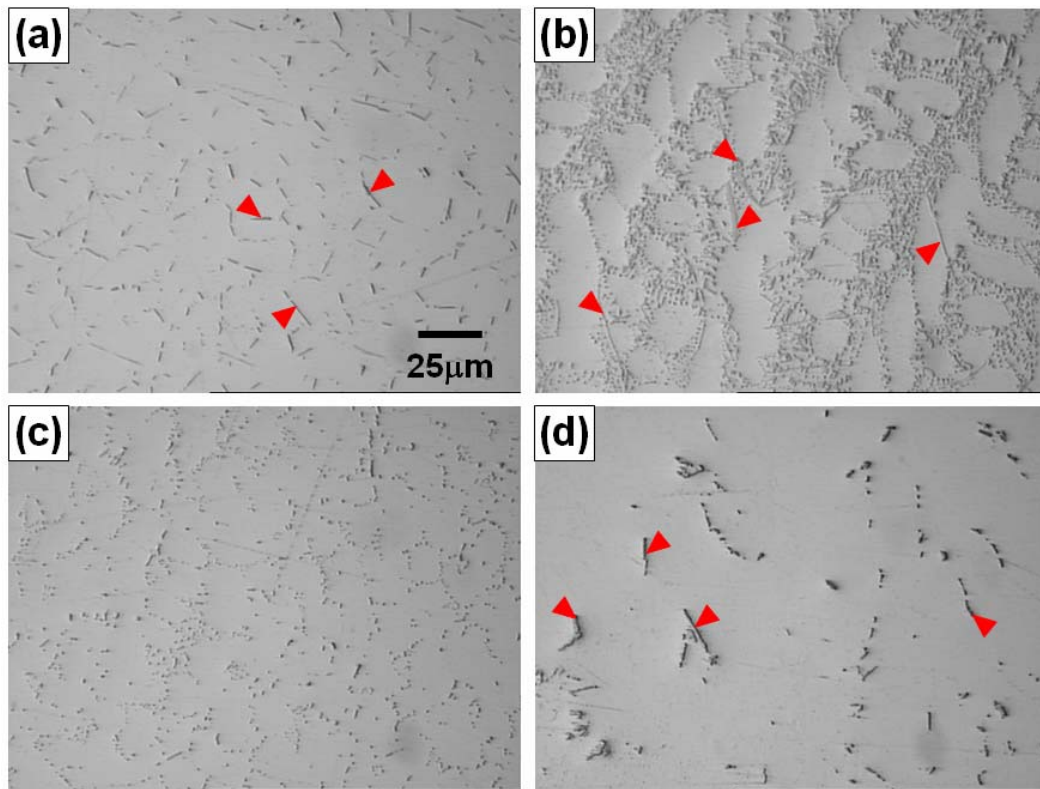


Figure 8. OM images inside (a) Sn-0.2Ni solder, (b) Sn-3.5Ag-0.15Ni solder, (c) Sn-0.7Cu-0.2Cu solder, and (d) Sn-0.7Cu-0.4Ni solder solidified at a cooling rate of  $6^{\circ}\text{C}/\text{min}$  during DSC.

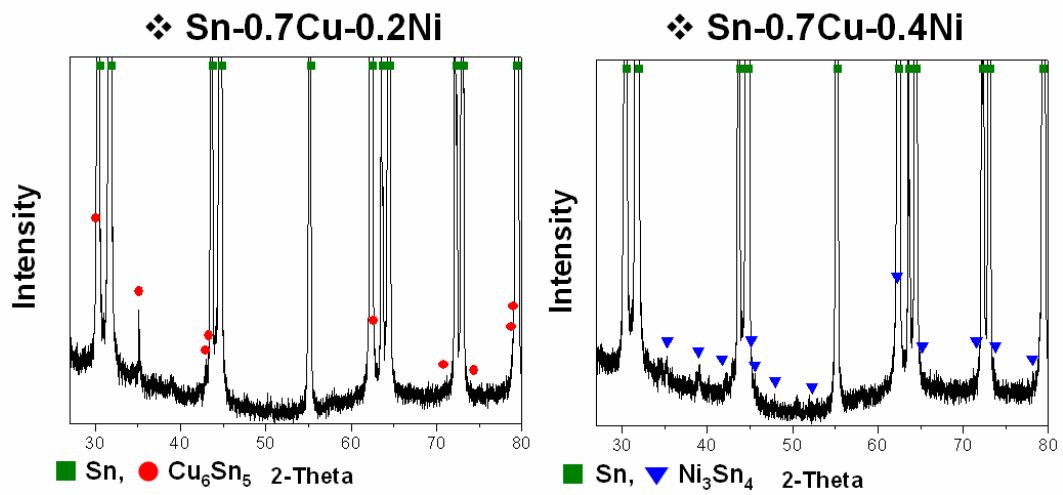


Figure 9. XRD patterns of Sn-0.7Cu-0.2N solder and Sn-0.7Cu-0.4Ni solder. Sn and  $\text{Cu}_6\text{Sn}_5$  IMCs were detected in the Sn-0.7Cu-0.2Ni solder and Sn and  $\text{Ni}_3\text{Sn}_4$  IMCs in the Sn-0.7Cu-0.4Ni solder.